Current Science
CS 5 (4), 4040-4058 (2025)
Received 15 May 2025 | **Revised 13 June** 2025 | **Accepted 10 July**. 2025 | **Online Available 17 August** 2025
https://doi.org/ 10.52845/CS/2025-5-4-56

Current Science
Current Science

OPEN ACCESS

ISSN (O) 2795-8639

Original Article

Mendelian Randomization Analysis between Micro RNA and Gastrointestinal Stromal Tumor

Qionglin Huang[1], Pengkhun Nov[1*], Jiqiang Li[1]*

[1]Department of Radiation Oncology, Oncology Center, Zhujiang Hospital, Southern Medical University, Guangzhou, Guangdong, 510282, P.R. China

[*]Corresponding Author: Jiqiang Li, Dr. Pengkhun Nov

Abstract:

Background: MicroRNAs (miRNAs) are key regulators of gene expression and have been implicated in the pathogenesis of various cancers, including gastrointestinal stromal tumors (GISTs). However, the causal relationship between specific miRNAs and GIST risk remains uncertain. Mendelian Randomization (MR) offers a robust approach to infer causality by leveraging genetic variants as instrumental variables.

Methods: We conducted a two-sample MR analysis using summary statistics from genome-wide association studies (GWAS) of 2083 circulating miRNA levels and GIST susceptibility. Single nucleotide polymorphisms (SNPs) strongly associated with miRNA expression were selected as instrumental variables. The causal effect estimates were obtained using inverse-variance weighted (IVW) methods, complemented by sensitivity analyses including MR-Egger and weighted median approaches to assess for pleiotropy and robustness.

Results: Our results identified suggestive evidence for a causal relationship between specific 87 miRNAs and GIST risk. Notably, the GIST risk was strongly associated with miR-23a-3p [odds ratio (OR) = 6.379, 95% confidence interval (CI) = 1.080 – 37.659, p = 0.040], miR-20b-5p (OR = 5.666, 95% CI = 1.185–27.083, p = 0.029), miR-608 (OR = 3.291, 95% CI = 1.530 – 7.078, p = 0.002), miR-125b-5p (OR = 2.450, 95% CI = 1.185–5.065, p = 0.015), miR-1322 (OR = 2.142, 95% CI = 1.235–3.713, p = 0.006), and miR-939-5p (OR = 1.864, 95% CI = 1.260–2.759, p = 0.001).

Conclusions: This MR study provides preliminary evidence supporting a potential causal role of certain miRNAs in GIST development. These findings could inform future functional studies and highlight miRNAs as potential biomarkers or therapeutic targets in GIST management. Further research with larger GWAS datasets is warranted to validate these associations.

Keyword : Gastrointestinal stromal tumor , MR, MicroRNA

1. Introduction

Gastrointestinal stromal tumor (GIST) is the most common mesenchymal neoplasm of the gastrointestinal tract, characterized by the proliferation of Cajal cells or their precursors [1]. Despite advances in surgical and targeted therapies, GIST remains a significant clinical challenge due to its potential for malignant transformation and metastasis, underscoring the need for a deeper understanding of its underlying molecular mechanisms [2].

MicroRNAs (miRNAs) are small, non-coding RNA molecules that play crucial roles in regulating gene expression post-transcriptionally. Aberrant miRNA expression has been implicated in various cancers, including GIST, where they may influence tumor initiation, progression, and response to therapy [3]. However, whether alterations in specific miRNAs are causally linked to GIST development remains unclear, as most existing studies are observational and susceptible to confounding and reverse causation [4]. Mendelian randomization (MR) offers a powerful

epidemiological approach to infer causal relationships by utilizing genetic variants as instrumental variables for exposures, such as miRNA levels. This method minimizes confounding and reverse causation, providing more robust evidence for causality [5].

In this study, we aim to investigate the causal relationship between circulating microRNAs and the risk of GIST through a Mendelian randomization framework. Elucidating these causal links could enhance our understanding of GIST pathogenesis and identify potential microRNA-based biomarkers or therapeutic targets.

2. Method

2.1 Study Design

To explore the causal relationships of miRNAs on gastrointestinal stromal tumors (GIST), a two-sample Mendelian randomization (MR) was performed using instrumental variables (IVs) extracted from a large-scale investigation of the genetics of miRNAs [6]. Multiple GIST-related phenotypes from GWAS were used as outcomes. The MR design is based on three assumptions: (1) genetic variants are robustly associated with exposure data (miRNA expression levels); (2) genetic variants are not associated with potential confounders; (3) genetic variants affect the outcome only through the exposure of interest [7]. In this study, multiple methods were used for MR and sensitivity analyses to confirm the robustness of the results **Figure 1**.

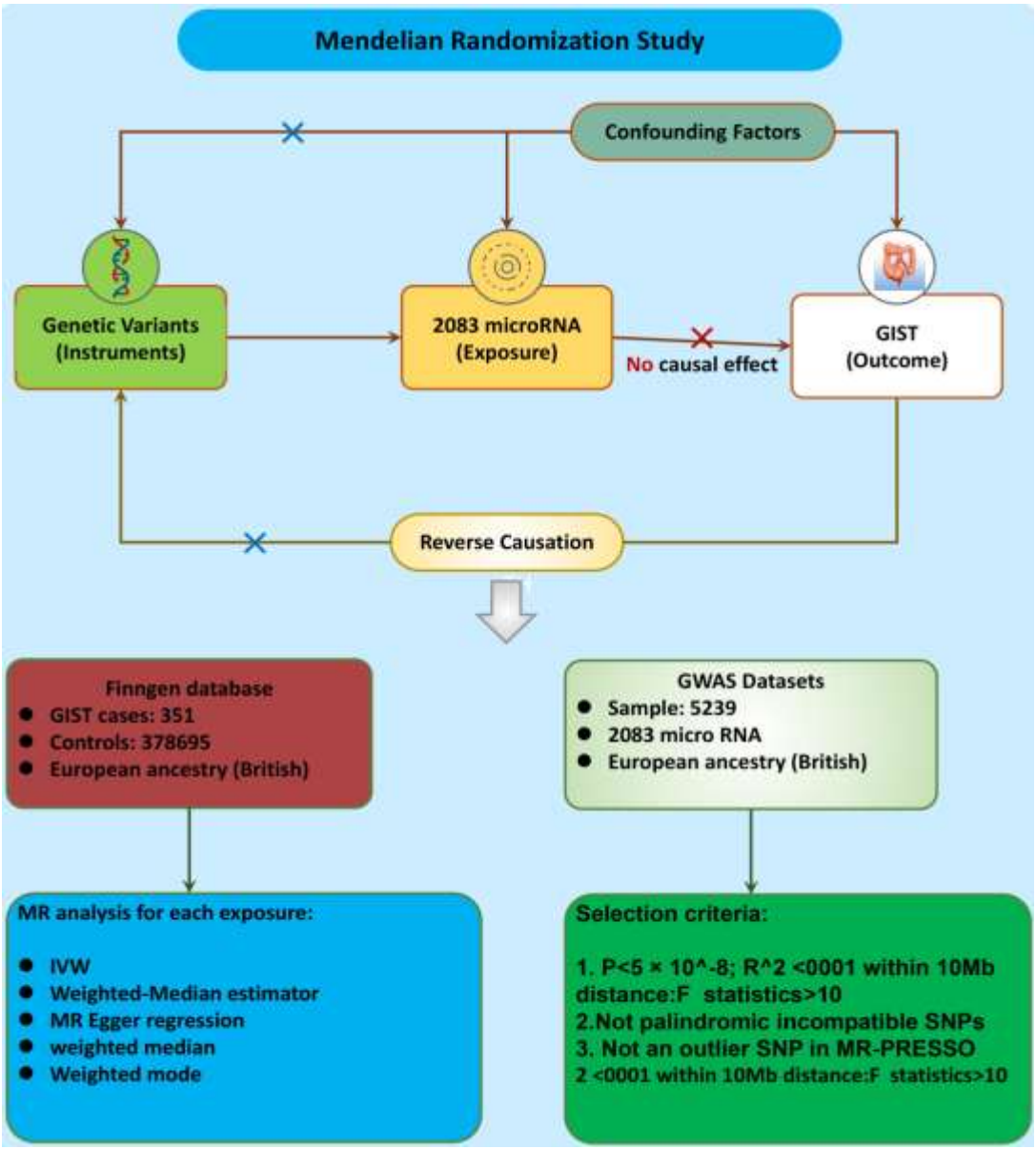

Figure 1 Study Design Flowchart

2.2 Exposure Data

In this study, we used large-scale miRNA expression quantitative trait loci (eQTLs) data as our exposure. We obtained the miRNA eQTL data from a previous study, which can be accessed from the Genome-Wide Association Study (GWAS) summary statistics database (https://gwas.mrcieu.ac.uk/). This study comprehensively examined genetic variants associated with the expression levels of 76 mature human miRNAs using a sample of 5,239 participants from the Framingham Heart Study (FHS). Age, sex, and cohort differences were corrected during the analysis, and a total of 9,612 variants were identified with a false discovery rate (FDR) of less than 0.1.

2.3 Outcome Data

To comprehensively study the causal effect of miRNAs on GIST, we collected GWAS summary statistics of multiple GIST-related phenotypes. We retrieved genetic data for GIST risk from the latest GWAS, including 379046 sample size (351 cases, and 378695 controls.

2.4 Selection Criteria of Instrumental Variables

In line with the three assumptions stated in the study design, quality control was performed on single nucleotide polymorphisms (SNPs) to ensure the robustness of the results. Similar to most current MR studies, the genome-wide significance threshold ($p < 5 \times 10^{-8}$) was selected to screen SNPs. Due to the limited number of SNPs meeting the genome-wide significance criteria, we used SNPs with a more relaxed threshold ($p < 1 \times 10^{-5}$) as potential IVs for each miRNA. To ensure independence among IVs, we applied linkage disequilibrium clumping with a clumping window of 10 MB and $R^2 < 0.001$ based on European ancestry reference data from the 1,000 Genomes Project. Meanwhile, to avoid bias caused by the employment of weak instruments, F statistics were calculated for each SNP to measure the statistical strength, and only strong IVs (F-statistics > 10) for each exposure were retained. Ambiguous and palindromic SNPs whose effects cannot be corrected in the harmonizing process were excluded. Since MR frequently generates false positives in the presence of genetic correlation between traits, SNPs associated with the outcome (GIST) were removed.

2.5 Mendelian Randomization Analyses

If there were two or more IVs, three different MR methods, namely random-effect inverse-variance weighted (IVW), MR Egger, and weighted median and Weighted mode, were performed to estimate the causal effect of miRNAs on GIST. IVW estimates were used as the main analysis, which combined the Wald ratio of each SNP on the outcome and obtained a pooled causal estimate. If horizontal pleiotropy was not present, the IVW results would be unbiased [8]. Meanwhile, MR-Egger and weighted median were used to improve the IVW estimates as they could provide more robust estimates in a broader set of scenarios, despite being less efficient (with wider confidence intervals). MR-Egger allows all genetic variants to have a pleiotropic effect but requires that the pleiotropic effects be independent of the variant-exposure association [9]. The weighted median method allows for the correct estimation of causal association when up to 50% of instrumental variables are invalid [10]. If only one IV was available, the Wald ratio method was used for MR analysis.

2.6 Sensitivity Analysis

Sensitivity analyses were conducted to identify underlying pleiotropy and heterogeneity, given their potential to significantly distort Mendelian randomization (MR) estimates. Heterogeneity was assessed using Cochran's Q test [11], with a p-value > 0.05 indicating the absence of statistically significant heterogeneity. Initial evaluation of pleiotropy was performed via the intercept term of MR Egger regression, where a p-value < 0.05 suggested potential pleiotropic effects among instrumental variables [12]. The MR-Pleiotropy Residual Sum and Outlier (MR-PRESSO) method was additionally employed to quantify and rectify horizontal pleiotropy [13]. Furthermore, a leave-one-out analysis was implemented to examine whether individual SNPs unduly influenced or biased the MR estimates. All the analyses were performed using the Two-Sample MR package in the R program (4.3.2).

3. Results

o assess the causal impact of various microRNA on GIST, the IVW method was employed for a two-sample MR analysis. The assessment results showed that 87 microRNA were association with GIST (**Figure 2, Figure 3**).

Exposure	Method	No.of SNP	OR(95% CI)	P
miR−301a−3p	Inverse variance weighted	6	0.266 (0.096 to 0.736)	0.011
miR−212−3p	Inverse variance weighted	5	0.313 (0.149 to 0.655)	0.002
miR−6795−3p	Inverse variance weighted	11	0.332 (0.121 to 0.912)	0.033
miR−3141	Inverse variance weighted	16	0.380 (0.155 to 0.932)	0.035
miR−6819−5p	Inverse variance weighted	9	0.385 (0.178 to 0.831)	0.015
miR−1265	Inverse variance weighted	6	0.443 (0.201 to 0.979)	0.044
miR−548h−5p	Inverse variance weighted	5	0.452 (0.243 to 0.841)	0.012
miR−200a−5p	Inverse variance weighted	7	0.457 (0.243 to 0.860)	0.015
miR−16−5p	Inverse variance weighted	33	0.463 (0.214 to 0.999)	0.050
miR−6778−5p	Inverse variance weighted	10	0.479 (0.259 to 0.885)	0.019
miR−192−3p	Inverse variance weighted	6	0.482 (0.247 to 0.938)	0.032
miR−3175	Inverse variance weighted	6	0.514 (0.289 to 0.915)	0.024
miR−4427	Inverse variance weighted	7	0.515 (0.297 to 0.896)	0.019
miR−19b−1−5p	Inverse variance weighted	13	0.541 (0.314 to 0.930)	0.026
miR−193b−3p	Inverse variance weighted	8	0.559 (0.314 to 0.996)	0.048
miR−6771−5p	Inverse variance weighted	11	0.565 (0.355 to 0.901)	0.017
miR−4504	Inverse variance weighted	7	0.577 (0.349 to 0.954)	0.032
miR−4261	Inverse variance weighted	11	0.582 (0.355 to 0.956)	0.033
miR−362−3p	Inverse variance weighted	14	0.584 (0.351 to 0.970)	0.038
let−7e−3p	Inverse variance weighted	7	0.596 (0.370 to 0.961)	0.034
miR−6736−5p	Inverse variance weighted	19	0.603 (0.440 to 0.827)	0.002
miR−3179	Inverse variance weighted	9	0.605 (0.371 to 0.986)	0.044
miR−514b−5p	Inverse variance weighted	13	0.606 (0.414 to 0.886)	0.010
miR−551b−5p	Inverse variance weighted	15	0.606 (0.373 to 0.984)	0.043
miR−1270	Inverse variance weighted	15	0.611 (0.401 to 0.929)	0.021
miR−1238−5p	Inverse variance weighted	13	0.613 (0.417 to 0.900)	0.013
miR−1305	Inverse variance weighted	14	0.614 (0.451 to 0.835)	0.002
miR−631	Inverse variance weighted	10	0.614 (0.402 to 0.937)	0.024
miR−758−5p	Inverse variance weighted	9	0.617 (0.387 to 0.983)	0.042
miR−8088	Inverse variance weighted	14	0.662 (0.486 to 0.902)	0.009
miR−4748	Inverse variance weighted	12	0.667 (0.467 to 0.953)	0.026
miR−1275	Inverse variance weighted	21	0.682 (0.469 to 0.993)	0.046
miR−6508−5p	Inverse variance weighted	15	0.692 (0.492 to 0.972)	0.034
miR−4709−3p	Inverse variance weighted	16	0.697 (0.488 to 0.996)	0.048
miR−3681−5p	Inverse variance weighted	12	0.722 (0.536 to 0.973)	0.032
miR−3182	Inverse variance weighted	15	0.724 (0.546 to 0.959)	0.024
miR−7978	Inverse variance weighted	20	0.743 (0.557 to 0.991)	0.043
miR−1264	Inverse variance weighted	11	0.752 (0.570 to 0.994)	0.045

Figure 2. The causal association between 6 microRNAs and GIST for risk factor

Exposure	Method	No.of SNP	OR(95% CI)	P
miR−4531	Inverse variance weighted	14	1.370 (1.027 to 1.827)	0.032
miR−6881−3p	Inverse variance weighted	13	1.389 (1.045 to 1.847)	0.024
miR−627−3p	Inverse variance weighted	12	1.390 (1.023 to 1.889)	0.035
miR−604	Inverse variance weighted	20	1.393 (1.084 to 1.790)	0.010
miR−513a−5p	Inverse variance weighted	13	1.405 (1.020 to 1.935)	0.037
miR−617	Inverse variance weighted	8	1.444 (1.030 to 2.023)	0.033
miR−27a−5p	Inverse variance weighted	16	1.451 (1.055 to 1.996)	0.022
miR−6810−5p	Inverse variance weighted	16	1.462 (1.020 to 2.096)	0.039
miR−522−3p	Inverse variance weighted	11	1.465 (1.097 to 1.958)	0.010
miR−6838−3p	Inverse variance weighted	17	1.470 (1.060 to 2.038)	0.021
miR−4686	Inverse variance weighted	11	1.471 (1.040 to 2.080)	0.029
miR−1185−5p	Inverse variance weighted	14	1.471 (1.051 to 2.059)	0.024
miR−494−5p	Inverse variance weighted	11	1.472 (1.048 to 2.068)	0.026
miR−1252−5p	Inverse variance weighted	12	1.480 (1.068 to 2.050)	0.018
miR−202−5p	Inverse variance weighted	8	1.518 (1.004 to 2.295)	0.048
miR−6876−3p	Inverse variance weighted	11	1.540 (1.053 to 2.252)	0.026
miR−3974	Inverse variance weighted	14	1.568 (1.043 to 2.357)	0.031
miR−5002−5p	Inverse variance weighted	11	1.591 (1.017 to 2.488)	0.042
miR−6848−3p	Inverse variance weighted	12	1.631 (1.147 to 2.318)	0.006
miR−4656	Inverse variance weighted	14	1.632 (1.114 to 2.392)	0.012
miR−4251	Inverse variance weighted	14	1.636 (1.149 to 2.329)	0.006
miR−6828−5p	Inverse variance weighted	5	1.645 (1.030 to 2.626)	0.037
miR−6889−3p	Inverse variance weighted	9	1.652 (1.063 to 2.566)	0.026
miR−760	Inverse variance weighted	11	1.690 (1.029 to 2.775)	0.038
miR−4314	Inverse variance weighted	8	1.694 (1.004 to 2.860)	0.048
miR−507	Inverse variance weighted	9	1.713 (1.086 to 2.704)	0.021
miR−331−5p	Inverse variance weighted	10	1.718 (1.041 to 2.836)	0.034
miR−514a−5p	Inverse variance weighted	7	1.728 (1.057 to 2.824)	0.029
miR−548k	Inverse variance weighted	9	1.759 (1.151 to 2.687)	0.009
miR−4791	Inverse variance weighted	7	1.780 (1.165 to 2.720)	0.008
miR−2276−3p	Inverse variance weighted	6	1.809 (1.002 to 3.266)	0.049
miR−2682−5p	Inverse variance weighted	11	1.843 (1.085 to 3.131)	0.024
miR−939−5p	Inverse variance weighted	10	1.865 (1.260 to 2.759)	0.002
miR−7158−3p	Inverse variance weighted	10	1.883 (1.288 to 2.752)	0.001
miR−3126−3p	Inverse variance weighted	7	1.966 (1.159 to 3.334)	0.012
miR−7851−3p	Inverse variance weighted	9	2.016 (1.322 to 3.074)	0.001
miR−4733−3p	Inverse variance weighted	4	2.138 (1.021 to 4.475)	0.044
miR−1322	Inverse variance weighted	11	2.142 (1.236 to 3.714)	0.007
miR−6768−5p	Inverse variance weighted	8	2.183 (1.170 to 4.074)	0.014
miR−6802−5p	Inverse variance weighted	13	2.389 (1.130 to 5.049)	0.023
miR−125b−5p	Inverse variance weighted	13	2.450 (1.185 to 5.065)	0.016
miR−6771−3p	Inverse variance weighted	5	2.492 (1.014 to 6.121)	0.047
miR−4793−5p	Inverse variance weighted	8	2.493 (1.245 to 4.993)	0.010
miR−3197	Inverse variance weighted	5	2.623 (1.062 to 6.476)	0.037
miR−6789−3p	Inverse variance weighted	5	3.211 (1.259 to 8.189)	0.015
miR−608	Inverse variance weighted	3	3.291 (1.530 to 7.078)	0.002
miR−23b−3p	Inverse variance weighted	14	5.305 (1.027 to 27.419)	0.046
miR−20b−5p	Inverse variance weighted	7	5.667 (1.186 to 27.083)	0.030
miR−23a−3p	Inverse variance weighted	13	6.380 (1.081 to 37.659)	0.041

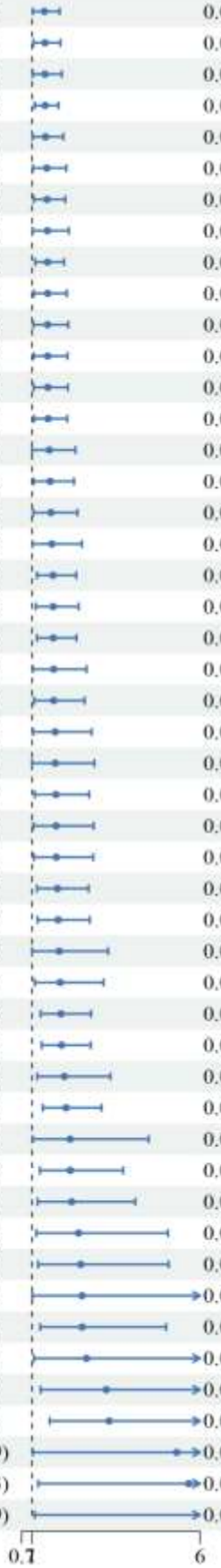

Figure 3. The causal association between microRNAs and GIST for protective factor with GIST. We selected Inverse variance weighted (IVW) as a primary method p<0.05 showed statistically significant; OR value >1 indicated a risk factor, while OR value <1 indicated a protective factor.

Briefly, the GIST risk was strongly associated with miR-23a-3p [odds ratio (OR) = 6.379, 95% confidence interval (CI) = 1.080 – 37.659, p = 0.040], miR-20b-5p (OR = 5.666, 95% CI = 1.185– 27.083, p = 0.029), miR-608 (OR = 3.291, 95% CI = 1.530 – 7.078, p = 0.002), miR-125b-5p (OR = 2.450, 95% CI = 1.185–5.065, p = 0.015), miR-1322 (OR = 2.142, 95% CI = 1.235–3.713, p = 0.006), and miR-939-5p (OR = 1.864, 95% CI = 1.260–2.759, p = 0.001) (**Figure 4**).

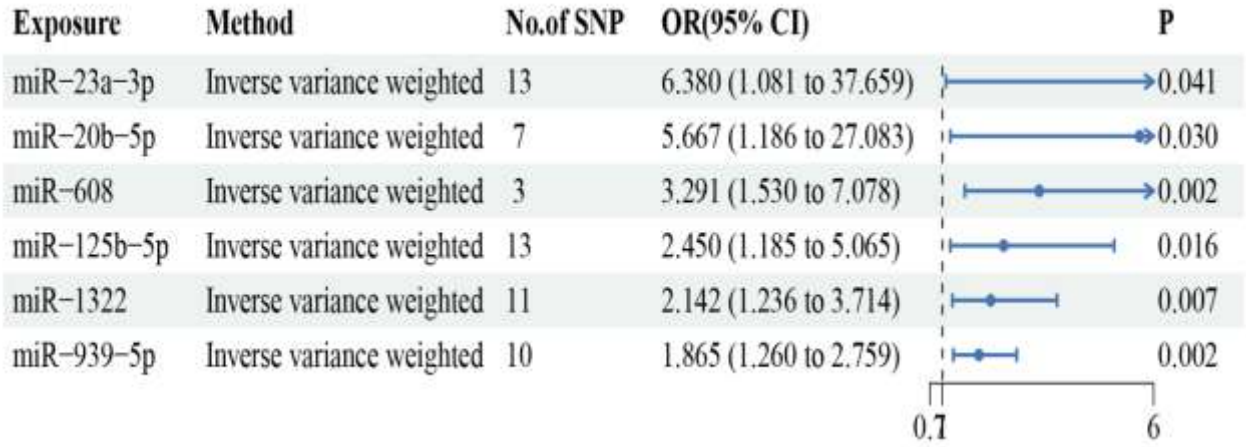

Figure 4. The causal association between microRNAs and GIST risk. We selected Inverse variance weighted (IVW) as a primary method p<0.05 showed statistically significant; OR value >1 indicated a risk factor, while OR value <1 indicated a protective factor.

Furthermore, the results of the sensitivity analysis are summarized herein. Although heterogeneity was observed, with Cochran's Q test yielding a p-value less than 0.05, the causal estimates remained reliable when using a random-effects inverse-variance weighted (IVW) approach. Additionally, the p-values for the MR-Egger intercept exceeded 0.05, indicating no significant evidence of horizontal pleiotropy affecting the results (**Table SI, SII**). Additionally, we further evaluated the data using scatter plots (**Fig. 5A-F**), funnel plots (**Fig. 6A-F**), which helped to eliminate the potential influence of outliers and horizontal pleiotropy on the identified key microRNA.

Table SI The heterogeneity of causal association between all microRNAs and GIST. The p-values for the Cochran's Q yielded were above 0.05, suggesting that no significant heterogeneity effects were found.

Exposure	Method	Q	Q_df	Q_pval
miR-25-3p	MR Egger	4.206889884	2	0.122035299
miR-7978	MR Egger	24.30001617	18	0.145442413
miR-19b-1-5p	Inverse variance weighted	17.1007149	12	0.145847869
miR-7978	Inverse variance weighted	25.40390527	19	0.147672286
miR-3974	MR Egger	16.9934664	12	0.149843248
miR-1265	MR Egger	6.696622026	4	0.152815569
miR-23b-3p	MR Egger	16.54479501	12	0.167537533
miR-3974	Inverse variance weighted	17.71821871	13	0.168514545
miR-19b-1-5p	MR Egger	15.16828657	11	0.174921605
miR-25-3p	Inverse variance weighted	4.94882197	3	0.175583239
miR-6838-3p	MR Egger	19.14862333	15	0.207077846
miR-23b-3p	Inverse variance weighted	16.63361362	13	0.216598914
miR-4261	Inverse variance weighted	12.93421094	10	0.227373459
miR-4261	MR Egger	11.72069774	9	0.229516895

miR-6810-5p	MR Egger	17.37268349	14	0.236860944
miR-1265	Inverse variance weighted	6.713801773	5	0.242810036
miR-6736-5p	Inverse variance weighted	21.40789833	18	0.259335615
miR-6838-3p	Inverse variance weighted	19.17821962	16	0.2595297
miR-6810-5p	Inverse variance weighted	17.9767691	15	0.26388885
miR-658	MR Egger	2.638099718	2	0.267389239
miR-6819-5p	MR Egger	8.712516128	7	0.273960439
miR-4709-3p	Inverse variance weighted	17.78265243	15	0.274264545
miR-4709-3p	MR Egger	16.65642995	14	0.274949379
miR-6508-5p	Inverse variance weighted	16.54723192	14	0.281109169
miR-513a-5p	MR Egger	12.81755294	11	0.305417192
miR-507	MR Egger	8.29236749	7	0.307520605
miR-604	MR Egger	20.41854596	18	0.309755256
miR-6876-3p	Inverse variance weighted	11.53505021	10	0.317377661
miR-4531	Inverse variance weighted	14.73644037	13	0.324093948
miR-658	Inverse variance weighted	3.455275313	3	0.326609257
miR-6795-3p	Inverse variance weighted	11.38654078	10	0.328206171
miR-6508-5p	MR Egger	14.57906526	13	0.334362216
miR-125b-5p	MR Egger	12.37331953	11	0.336245957
miR-507	Inverse variance weighted	9.015888227	8	0.340957417
miR-6795-3p	MR Egger	10.05552046	9	0.34600925
miR-3681-5p	MR Egger	11.08397985	10	0.351012754
miR-6876-3p	MR Egger	9.954968085	9	0.354143107
miR-4531	MR Egger	13.14790747	12	0.358382468
miR-608	Inverse variance weighted	2.036753	2	0.361180842
miR-6819-5p	Inverse variance weighted	8.744758838	8	0.364283313
miR-604	Inverse variance weighted	20.45163431	19	0.36787537
miR-6778-5p	MR Egger	8.703606496	8	0.367912965
miR-3179	Inverse variance weighted	8.659375772	8	0.371840078
miR-2276-3p	MR Egger	4.250963646	4	0.373105757
miR-6736-5p	MR Egger	18.14918718	17	0.379488069
miR-513a-5p	Inverse variance weighted	12.81933767	12	0.382307683
miR-3179	MR Egger	7.442054246	7	0.384347092
miR-1270	Inverse variance weighted	14.57590706	14	0.407744583
miR-125b-5p	Inverse variance weighted	12.39191853	12	0.414739337
miR-4504	Inverse variance weighted	6.051932971	6	0.417397751
miR-3681-5p	Inverse variance weighted	11.16998078	11	0.429134734
miR-6802-5p	Inverse variance weighted	12.1540842	12	0.433385679
miR-1322	MR Egger	8.90107932	9	0.446455179
miR-548h-5p	Inverse variance weighted	3.678738071	4	0.4512259
miR-6778-5p	Inverse variance weighted	8.83686799	9	0.452467104
miR-617	MR Egger	5.626210496	6	0.466335578
miR-1270	MR Egger	12.7406199	13	0.468040723
miR-1322	Inverse variance weighted	9.690273728	10	0.468073849
miR-4748	MR Egger	9.674745648	10	0.469477238
miR-608	MR Egger	0.51514817	1	0.472918705
miR-6889-3p	MR Egger	6.516670372	7	0.480873194
miR-2276-3p	Inverse variance weighted	4.467876854	5	0.484192876
miR-4314	Inverse variance weighted	6.484093129	7	0.484491784
miR-548h-5p	MR Egger	2.417289511	3	0.490424301

miR-5002-5p	MR Egger	8.412551745	9	0.493163857
miR-212-3p	Inverse variance weighted	3.38497669	4	0.495581953
miR-4314	MR Egger	5.30381885	6	0.505477432
miR-4251	MR Egger	11.26083538	12	0.506707254
miR-494-5p	MR Egger	8.242452841	9	0.509909688
miR-212-3p	MR Egger	2.311976644	3	0.510230384
miR-4656	MR Egger	11.19484371	12	0.512298538
miR-1252-5p	MR Egger	9.19352935	10	0.513840842
miR-4748	Inverse variance weighted	10.11652951	11	0.519936743
miR-6768-5p	MR Egger	5.159298095	6	0.523550485
miR-20b-5p	MR Egger	4.169915336	5	0.525220837
miR-6889-3p	Inverse variance weighted	7.081226182	8	0.527894911
miR-362-3p	MR Egger	10.93717643	12	0.534310236
miR-1252-5p	Inverse variance weighted	9.847642268	11	0.544141792
miR-4251	Inverse variance weighted	11.71414068	13	0.551212119
miR-5002-5p	Inverse variance weighted	8.78401341	10	0.552716965
miR-617	Inverse variance weighted	5.835520334	7	0.55908092
miR-494-5p	Inverse variance weighted	8.644142043	10	0.566175486
miR-4656	Inverse variance weighted	11.46208848	13	0.572166407
miR-362-3p	Inverse variance weighted	11.21557075	13	0.592764007
miR-4427	MR Egger	3.683549698	5	0.595813906
miR-939-5p	MR Egger	6.336216285	8	0.609626087
miR-6768-5p	Inverse variance weighted	5.412991185	7	0.609698461
miR-4504	MR Egger	3.586920735	5	0.61027815
miR-514a-5p	Inverse variance weighted	4.416363446	6	0.620520699
miR-20b-5p	Inverse variance weighted	4.35781947	6	0.628374221
miR-939-5p	Inverse variance weighted	6.997058492	9	0.637425676
miR-4791	MR Egger	3.398478753	5	0.638801623
miR-4686	Inverse variance weighted	7.895789833	10	0.63901538
miR-4793-5p	MR Egger	4.257416656	6	0.641885407
miR-192-3p	MR Egger	2.514040561	4	0.64212339
miR-3175	Inverse variance weighted	3.37352867	5	0.642604648
miR-1185-5p	MR Egger	9.590047434	12	0.65187594
miR-7851-3p	MR Egger	5.06199676	7	0.652397532
miR-758-5p	MR Egger	5.037142249	7	0.655430437
miR-6828-5p	MR Egger	1.593535918	3	0.660856394
miR-7158-3p	MR Egger	5.644031777	8	0.687035553
miR-4793-5p	Inverse variance weighted	4.773903971	7	0.687532297
miR-6802-5p	MR Egger	8.229128511	11	0.69264368
miR-514a-5p	MR Egger	3.028569397	5	0.695581096
miR-2682-5p	Inverse variance weighted	7.182565594	10	0.70810456
miR-6848-3p	MR Egger	7.16786523	10	0.709508111
miR-7851-3p	Inverse variance weighted	5.434278403	8	0.710310011
miR-4427	Inverse variance weighted	3.683551275	6	0.719410219
miR-1185-5p	Inverse variance weighted	9.591587021	13	0.726941813
miR-4791	Inverse variance weighted	3.623586036	6	0.727461077
miR-3126-3p	MR Egger	2.789329312	5	0.732425648
miR-4686	MR Egger	6.032341312	9	0.736677118
miR-1264	Inverse variance weighted	6.816000086	10	0.742693998
miR-2682-5p	MR Egger	5.970214058	9	0.742895663

miR-7158-3p	Inverse variance weighted	5.955783332	9	0.74433541
miR-3197	MR Egger	1.208556764	3	0.750952786
miR-331-5p	MR Egger	5.051588166	8	0.752048358
miR-758-5p	Inverse variance weighted	5.043498184	8	0.752917031
miR-3182	MR Egger	9.043911137	13	0.769619093
miR-6828-5p	Inverse variance weighted	1.81494468	4	0.769747025
miR-760	Inverse variance weighted	6.473023975	10	0.774080786
miR-192-3p	Inverse variance weighted	2.51448215	5	0.774312469
miR-6848-3p	Inverse variance weighted	7.281829016	11	0.775822744
miR-6771-3p	MR Egger	1.098365934	3	0.777468568
miR-3175	MR Egger	1.760481031	4	0.779704082
miR-1305	MR Egger	7.86836669	12	0.795330621
miR-3141	MR Egger	9.50152228	14	0.797645171
miR-6771-5p	MR Egger	5.391428387	9	0.798939431
miR-514b-5p	Inverse variance weighted	7.757423233	12	0.803788042
miR-3126-3p	Inverse variance weighted	3.014660654	6	0.807004526
miR-23a-3p	Inverse variance weighted	7.664933777	12	0.810736109
miR-6881-3p	MR Egger	6.843305988	11	0.811627191
miR-6789-3p	Inverse variance weighted	1.567721359	4	0.814581542
miR-8088	Inverse variance weighted	8.40399123	13	0.816321885
miR-514b-5p	MR Egger	6.764037496	11	0.81785761
miR-331-5p	Inverse variance weighted	5.126722409	9	0.823124537
miR-3182	Inverse variance weighted	9.044245666	14	0.82820579
miR-627-3p	MR Egger	5.836503187	10	0.828807324
miR-6789-3p	MR Egger	0.880187739	3	0.830206139
miR-27a-5p	MR Egger	8.996687653	14	0.831262709
miR-23a-3p	MR Egger	6.421946001	11	0.843781092
miR-3141	Inverse variance weighted	9.51060314	15	0.849344236
miR-1305	Inverse variance weighted	7.884305675	13	0.851054959
miR-627-3p	Inverse variance weighted	6.318023107	11	0.851324616
miR-1264	MR Egger	4.763350301	9	0.85443041
miR-6881-3p	Inverse variance weighted	6.946959377	12	0.861098694
miR-3197	Inverse variance weighted	1.301109792	4	0.861187211
miR-6771-5p	Inverse variance weighted	5.41982125	10	0.861429495
miR-193b-3p	MR Egger	2.551597717	6	0.862648955
miR-202-5p	MR Egger	2.516920881	6	0.866569163
miR-548k	Inverse variance weighted	3.8396755	8	0.871290951
miR-27a-5p	Inverse variance weighted	9.017673854	15	0.876591526
miR-6771-3p	Inverse variance weighted	1.207135541	4	0.876922406
miR-8088	MR Egger	6.576299353	12	0.884297889
miR-1238-5p	MR Egger	5.740641656	11	0.890096734
miR-760	MR Egger	4.27258698	9	0.89257313
miR-522-3p	MR Egger	4.22192835	9	0.896207842
miR-1238-5p	Inverse variance weighted	6.319281421	12	0.899139595
miR-193b-3p	Inverse variance weighted	2.79535817	7	0.903265985
let-7e-3p	Inverse variance weighted	2.095187431	6	0.910739244
let-7e-3p	MR Egger	1.489498618	5	0.914278481
miR-202-5p	Inverse variance weighted	2.566400266	7	0.922014619
miR-631	Inverse variance weighted	3.791926828	9	0.924565832
miR-631	MR Egger	3.106539489	8	0.927494648

miR-4733-3p	MR Egger	0.13529901	2	0.934587985
miR-522-3p	Inverse variance weighted	4.247068627	10	0.935513708
miR-301a-3p	MR Egger	0.689772344	4	0.952584185
miR-200a-5p	MR Egger	1.076618921	5	0.95615226
miR-301a-3p	Inverse variance weighted	0.993360452	5	0.963099519
miR-548k	MR Egger	1.738146124	7	0.972903952
miR-200a-5p	Inverse variance weighted	1.137312631	6	0.979867782
miR-16-5p	Inverse variance weighted	17.75491536	32	0.980249709
miR-1275	MR Egger	8.460540136	19	0.981406882
miR-4733-3p	Inverse variance weighted	0.156030717	3	0.984354271
miR-16-5p	MR Egger	16.17150358	31	0.986892194
miR-1275	Inverse variance weighted	8.522385296	20	0.987808188

Table SII The pleiotropy of causal association between all microRNAs and GIST. The p-values for the MR-Egger intercept were above 0.05, suggesting that no significant pleiotropy effects were found.

Exposure	Egger_intercept	Standard Error (Se)	P value
miR-6802-5p	-0.127226132	0.064218321	0.073125392
miR-6736-5p	0.110243672	0.0631008	0.098658556
miR-760	0.097719814	0.065876143	0.172122416
miR-4504	-0.160705887	0.102358107	0.177203085
miR-1264	0.086977416	0.06070844	0.185747106
miR-548k	-0.098376757	0.067861706	0.190430965
miR-1270	-0.099712351	0.073603241	0.198580889
miR-8088	0.105524775	0.078055398	0.201332184
miR-4686	0.08681478	0.063596757	0.205374791
miR-6508-5p	0.095169388	0.071838872	0.208066284
miR-16-5p	-0.091334099	0.072583184	0.217665075
miR-551b-5p	0.10577029	0.083532391	0.227654437
miR-4531	-0.06773973	0.05625784	0.251766791
miR-19b-1-5p	0.096030167	0.081119993	0.261441509
miR-6876-3p	-0.097453742	0.081537496	0.262551102
miR-3175	-0.133555599	0.105157076	0.272916897
miR-23a-3p	0.093011405	0.08342626	0.288661574
miR-514a-5p	-0.115403872	0.097962051	0.291787622
miR-2682-5p	-0.282094297	0.256200529	0.299441747
miR-6795-3p	0.113871422	0.104328611	0.303422644
miR-4314	0.117310525	0.107980543	0.319007164
miR-3179	-0.11651261	0.108884905	0.320098482
miR-514b-5p	-0.06652807	0.066749185	0.340336169
miR-548h-5p	-0.433898666	0.386325649	0.343148718
miR-4709-3p	-0.078659104	0.080846988	0.347095533
miR-4261	0.081422819	0.084348888	0.359609838
miR-212-3p	-0.133971301	0.12933376	0.376439598
miR-7978	0.051261822	0.05668894	0.377798863
miR-1322	0.079795721	0.08982301	0.397464655
miR-631	-0.066698751	0.080565603	0.431739517
miR-608	1.179692899	0.956352563	0.433677388
miR-1252-5p	-0.049499091	0.061202739	0.437464665
miR-939-5p	-0.089697959	0.110340176	0.439782941

miR-507	-0.082870421	0.106038677	0.460112739
miR-1238-5p	-0.05656534	0.074361179	0.462840415
miR-6789-3p	0.113144804	0.136454432	0.467816894
let-7e-3p	-0.06570208	0.084421749	0.471620243
miR-6889-3p	0.082761493	0.110147559	0.476926391
miR-3974	0.064130345	0.089643569	0.488052958
miR-6810-5p	0.049865572	0.071469541	0.496778766
miR-4793-5p	0.058077317	0.08081216	0.499361994
miR-627-3p	0.046734073	0.067348279	0.503534825
miR-4251	-0.04820526	0.071597693	0.513527907
miR-658	-0.088844927	0.112877023	0.513686456
miR-4748	-0.04622881	0.069551707	0.521294668
miR-494-5p	0.040764302	0.064318356	0.541988345
miR-5002-5p	-0.064399024	0.105662841	0.557279651
miR-7851-3p	0.062149535	0.101859625	0.561040615
miR-7158-3p	0.042835581	0.076718543	0.591886622
miR-362-3p	0.047992723	0.090958901	0.607373796
miR-301a-3p	0.087203232	0.158266939	0.610969047
miR-25-3p	-0.14980241	0.252233228	0.612803733
miR-4656	-0.036763907	0.071115956	0.614580887
miR-6768-5p	-0.097188314	0.19295664	0.632440946
miR-193b-3p	-0.046314245	0.093806508	0.639053731
miR-3126-3p	-0.055741115	0.117426157	0.655016343
miR-4791	0.044844253	0.094517456	0.655173375
miR-617	0.052138415	0.113962771	0.663407618
miR-6828-5p	0.052734024	0.112071069	0.670065438
miR-2276-3p	0.038165601	0.08447784	0.674839405
miR-20b-5p	0.040141886	0.092603969	0.682730979
miR-6778-5p	-0.066912844	0.191188505	0.735386473
miR-6848-3p	-0.027144395	0.080407532	0.742654959
miR-6881-3p	-0.021495824	0.066767074	0.753524234
miR-6771-3p	0.038885955	0.117906838	0.763235731
miR-3197	-0.042697589	0.140348584	0.780837968
miR-3681-5p	0.029561693	0.106126926	0.786264991
miR-331-5p	-0.023147501	0.08444718	0.790947629
miR-23b-3p	0.018774135	0.073968702	0.803937495
miR-1275	-0.022291711	0.089637668	0.80627129
miR-200a-5p	0.029629074	0.120266931	0.815197318
miR-202-5p	0.025813836	0.116048731	0.831350257
miR-604	0.011481211	0.06722429	0.866294348
miR-6771-5p	-0.01356169	0.080483937	0.869914515
miR-6819-5p	0.020738202	0.128848123	0.876678807
miR-522-3p	-0.010046762	0.063363783	0.87751882
miR-6838-3p	-0.011708567	0.076896804	0.881008375
miR-27a-5p	0.010116818	0.069835624	0.886881431
miR-4733-3p	-0.03858222	0.267959817	0.898710785
miR-125b-5p	0.009759347	0.075896659	0.900005105
miR-1305	-0.009928293	0.078640135	0.901624927
miR-1265	0.016736765	0.165219399	0.924186808

miR-3141	-0.008668393	0.090965163	0.925432224
miR-758-5p	0.008685305	0.108942005	0.938688012
miR-1185-5p	-0.002560978	0.065268514	0.96934622
miR-513a-5p	0.002854909	0.072947819	0.969482968
miR-192-3p	0.002743099	0.130536516	0.984240924
miR-3182	-0.001284524	0.070230408	0.985685133
miR-4427	-0.000182591	0.145426783	0.999046769

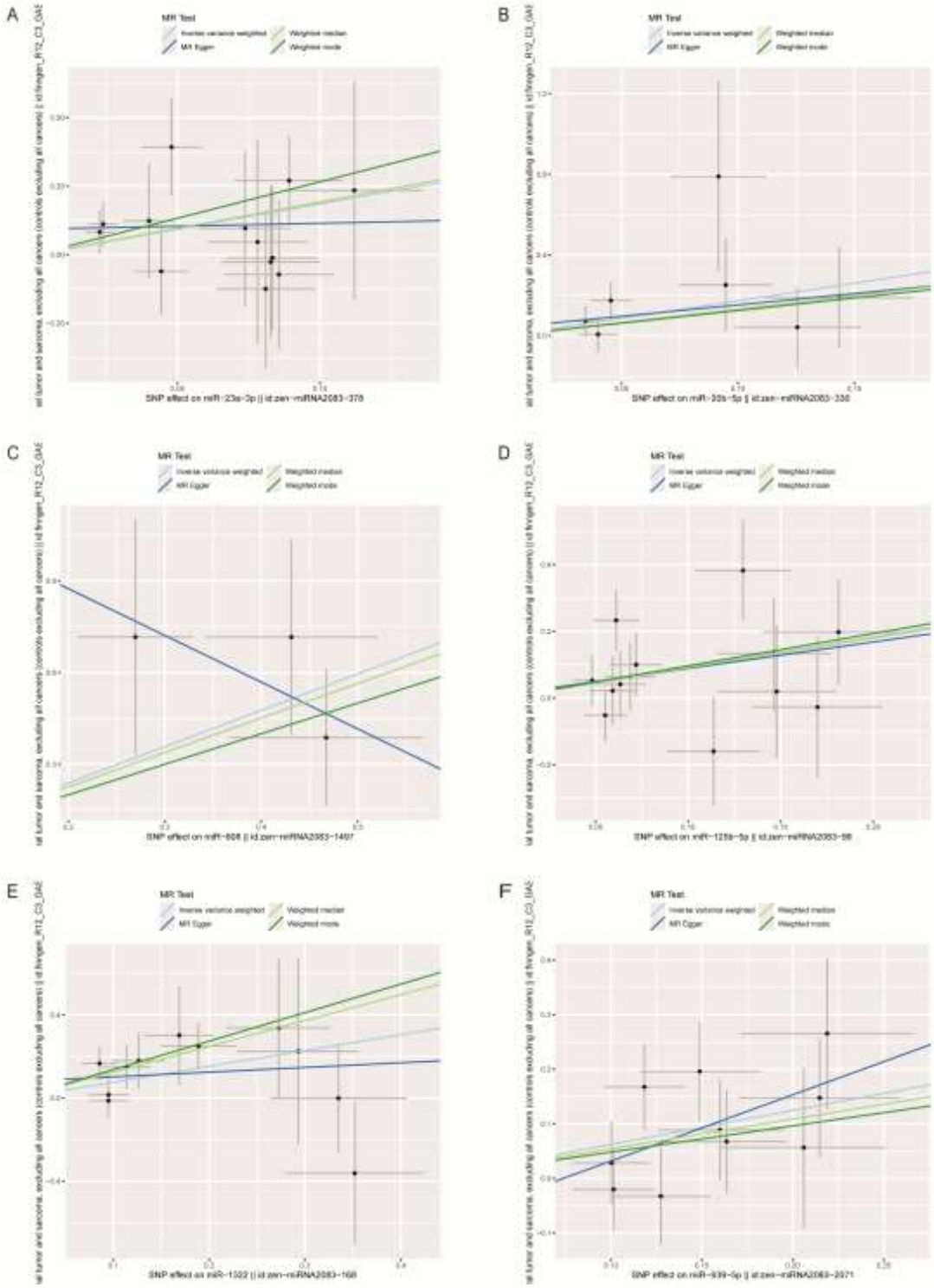

Figure 5. Scatter plot showing the relationship with the risk of GIST: (A) miR-23a-3p, (B) miR-125b-5p (B) miR-20b-5p, (C) miR-608, (D) miR-125b-5p, (E) miR-1322, and (F) miR-939-5p

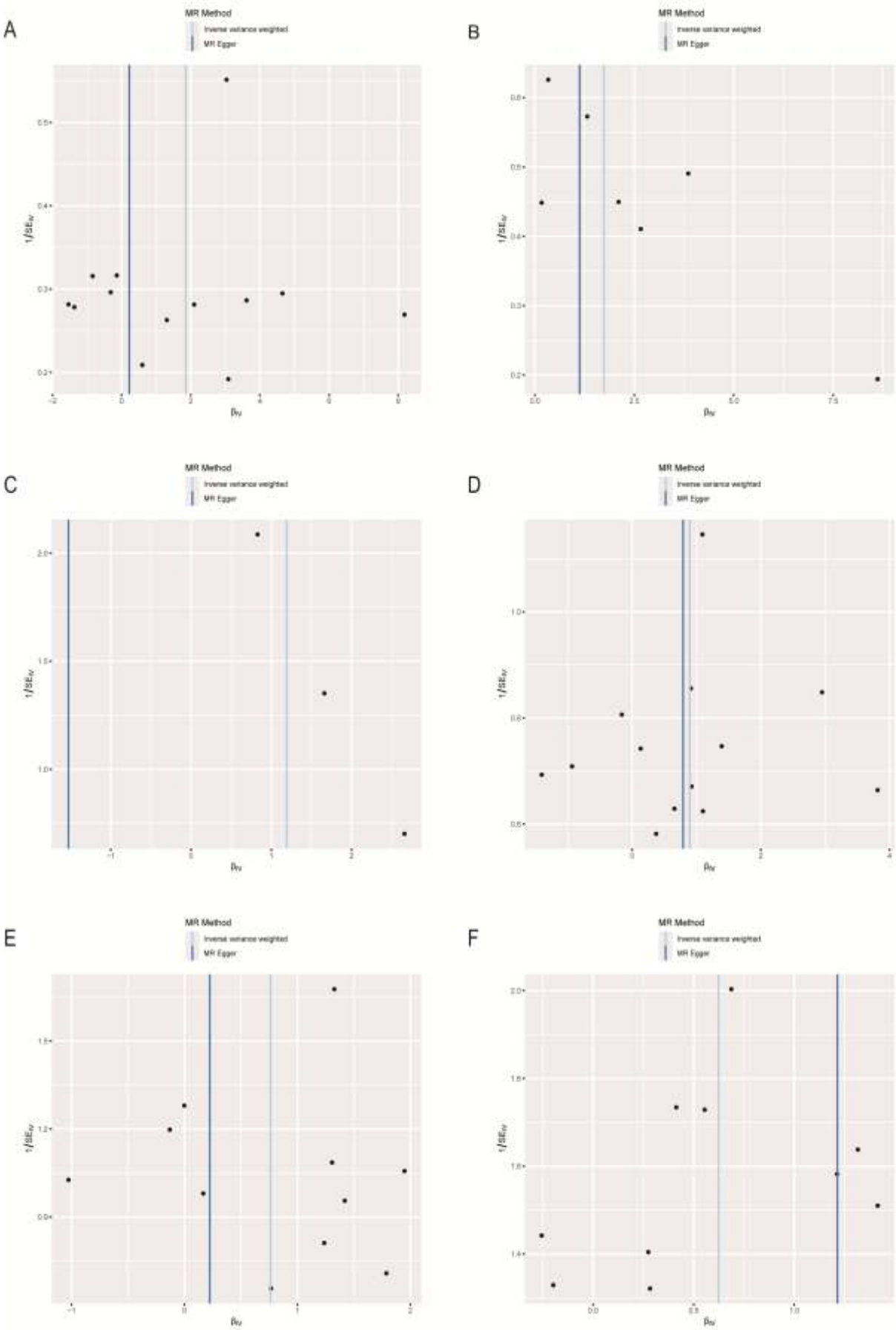

Figure 6. Funnel plot showing instrumental variables for each significant causal association between three miRNAs and GIST: (A) miR-23a-3p, (B) miR-125b-5p (B) miR-20b-5p, (C) miR-608, (D) miR-125b-5p, (E) miR-1322, and (F) miR-939-5p

4. Discussions

This study, through Mendelian randomization (MR) analysis, we found that 87 micro RNA were correlated with GIST. 38 miRNA serve as protective factor, while 49 miRNA were related with risk factor in GIST. We only address 6 miRNAs include miR-23a-3p, miR-20b-5p, miR-608, miR-125b-5p, miR-1322, and miR-939-5p in the progression of gastrointestinal stromal tumors (GIST)in the discussion sections. These miRNAs form a GIST-specific molecular regulatory network by targeting and regulating oncogenic signaling pathways, tumor microenvironment, and malignant cellular phenotypes, providing an important theoretical basis for elucidating the pathogenesis of GIST and developing novel diagnostic and therapeutic strategies.

miR-23a-3p exhibits differential regulatory effects in various malignant tumors. In melanoma, NEAT1 can drive tumor progression through the miR-23a-3p/KLF3 axis [14]. miR-23a-3p regulates the progression of colon cancer by inhibiting the expression of NDRG4 [15]. In hepatocellular carcinoma, endoplasmic reticulum stress-induced exosome transfer of miR-23a-3p upregulates PD-L1 expression through the PTEN/AKT pathway to suppress T-cell immunity, and is involved in regulating multiple biological processes such as cell cycle, apoptosis, metabolism, and ferroptosis (related to sorafenib resistance) [16-17]. These studies collectively reveal the multi-dimensional regulatory network of miR-23a-3p in tumorigenesis and development, as well as its potential value as a therapeutic target.

In the research on the mechanisms of tumorigenesis and development, the function of miR-20b-5p shows significant tumor type specificity and bidirectional regulatory characteristics. In solid tumors such as non-small cell lung cancer and nasopharyngeal carcinoma, this microRNA usually acts as an oncogenic factor, promoting tumor cell proliferation and metastasis by targeting tumor suppressor genes such as BTG3 and EGR1 [18-19]. However, in gastric cancer, it exerts a tumor-suppressive effect by inhibiting the PI3K/AKT/mTOR signaling pathway [20]. In prostate cancer, it inhibits the epithelial-mesenchymal transition (EMT) process by regulating the E-cadherin/vimentin axis [21]. This functional heterogeneity reveals that its biological effects are highly dependent on the tumor microenvironment and the differential expression patterns of downstream target genes. In hepatocellular carcinoma, miR-20b-5p is significantly upregulated, and its overexpression can significantly enhance the proliferation, migration, and invasion abilities of hepatocellular carcinoma cells [22]. Based on the evidence from multi-cancer studies, miR-20b-5p may act as a broad-spectrum oncogenic factor with environmental adaptability, participating in tumorigenesis and development by dynamically regulating different signaling pathways (including targeting tumor suppressor genes, inhibiting the PI3K/AKT/mTOR pathway, and regulating EMT, etc.). Its bidirectional functional mode provides an important molecular target for precise tumor treatment.

As a broad-spectrum tumor-suppressive microRNA, miR-608 shows characteristic low expression in various solid tumors except bladder cancer, and its tumor-suppressive function is mainly achieved by targeting and regulating core oncogene networks and inflammatory signaling pathways [23]. In chordoma and lung adenocarcinoma models, this molecule significantly inhibits tumor cell proliferation and induces apoptosis by directly binding to the 3' untranslated regions of EGFR, BCL-xL, and SHH gene mRNAs, confirming its negative regulatory role in the progression of malignant tumors [24-26]. A study revealed a new molecular mechanism by which miR-608 regulates monocyte inflammatory responses by targeting neutrophil elastase (ELANE). This breakthrough not only expands its functional dimension in the field of inflammatory regulation but also provides a highly potential therapeutic target for inflammatory-related diseases such as sepsis [26]. This research system systematically clarifies the dual biological functions of miR-608 in tumor suppression and inflammatory regulation, laying an important theoretical foundation for the development of multi-dimensional disease intervention strategies based on this molecule.

As a highly conserved member of the microRNA family, miR-125b-5p shows significantly low expression in various malignant tumors such as bladder cancer, breast cancer, and liver cancer, and its tumor-suppressive function is achieved

through multi-dimensional mechanisms. On the one hand, it directly targets the TPD52 gene, inhibits tumor cell proliferation, invasion, and epithelial-mesenchymal transition (EMT), induces cell apoptosis, enhances sensitivity to radiotherapy and chemotherapy, and is closely related to tumor grade, clinical stage, and patient prognosis [27-28]; on the other hand, it regulates the tumor immune microenvironment, inhibits the activation of γδ T cells and induces their apoptosis, and affects the expression of TNFR2 on the surface of regulatory T cells, participating in the construction of an immunosuppressive microenvironment [30]. Its expression level is affected by exogenous factors such as smoking (possibly regulated by NNK) and HPV infection, highlighting its potential value as a tumor therapeutic target [29]. Its complex expression regulatory network and bidirectional action mechanism (such as dual oncogenic/tumor-suppressive effects) in different tumor microenvironments need to be further studied to provide a theoretical basis for precise tumor treatment.

As an important tumor-suppressive microRNA, miR-1322 exerts anti-tumor effects in multiple cancer types through a complex molecular regulatory network. In liver cancer, its expression is regulated by the competitive endogenous adsorption of circular RNAs such as circ_0000291 and circ-HOMER1, and inhibits tumor cell proliferation and radio-chemotherapy resistance by targeting and negatively regulating the ubiquitin ligase UBE2T [31]. In colorectal cancer, the NF-κB pathway activated by Fusobacterium nucleatum infection regulates its expression, and participates in inflammation-driven tumorigenesis by targeting the chemokine CCL20 [32]. In prostate cancer, circSMARCC1 relieves its inhibition on CCL20 through sponge adsorption, thereby promoting tumor metastasis [33]. In esophageal cancer, it was found to target the tumor suppressor gene ECRG2 and show potential diagnostic marker value [34]. These studies reveal the multi-level tumor-suppressive network constructed by miR-1322 through the "epigenetic regulation-transcription factor-target gene network" (such as the circRNA-miR-1322-UBE2T/CCL20/ECRG2 axis), and its dysregulation is significantly related to malignant tumor phenotypes (proliferation, metastasis, treatment resistance). As a common therapeutic target for multiple cancer types, this molecule has the triple clinical value of "inhibiting tumor progression-reversing treatment resistance-predicting prognosis", providing a theoretical basis for the development of precise diagnosis and treatment strategies based on miR-1322.

miR-939-5p shows significant functional plasticity in tumorigenesis and development, and its expression pattern and regulatory effect are highly cancer-type specific. In pancreatic cancer, this microRNA activates the β-catenin/C-myc signaling axis by targeting ARHGAP4, and regulates Warburg metabolic reprogramming, thereby exerting an oncogenic effect [35]. In triple-negative breast cancer, its high expression negatively regulates tumor progression by inhibiting the NOS2/NOS3-NO pathway, and is significantly related to the poor prognosis of patients [36]. This molecule shows proliferation-promoting and anti-apoptotic properties in tongue squamous cell carcinoma [37], while inhibiting invasion and metastasis by targeting LIMK2 in colorectal cancer [38]. This functional contradiction stems from its spatio-temporally specific interaction network—the differential combination of upstream regulatory factors (such as HEIH long-chain RNA) and downstream effector molecules (ARHGAP4, NOS2, SLC34A2, etc.), forming regulatory modules with tumor microenvironment heterogeneity. The molecular regulatory network of miR-939-5p in specific cancer types needs to be combined with the intrinsic characteristics of tumor cells and microenvironmental features to systematically clarify its function conversion mechanism under different pathological conditions, providing a theoretical basis for the development of precise tumor diagnosis and treatment strategies based on miR-939-5p.

5. Strength and limitations

This study leverages the Mendelian Randomization approach to strengthen causal inference between miRNAs and GIST risk, minimizing confounding factors and reverse causation inherent in observational studies. The use of large-scale GWAS summary statistics enhances the statistical power and precision of the findings. Additionally, multiple sensitivity analyses, including MR-Egger and weighted median methods, were conducted to assess the robustness of the results and to detect potential

pleiotropy. The focus on genetic variants as instrumental variables provides a more reliable estimate of the causal relationship, offering novel insights into the potential biological role of specific miRNAs in GIST development. Overall, this approach provides a valuable framework for exploring molecular mechanisms underlying GISTs and identifying potential biomarkers or therapeutic targets.

Despite the strengths of this MR study, several limitations should be acknowledged. First, the number of valid genetic instruments (SNPs) associated with specific miRNAs was limited, which may reduce the statistical power and affect the robustness of causal inferences. Second, heterogeneity among instrumental variables was observed, and although sensitivity analyses such as MR-Egger indicated minimal pleiotropy, residual pleiotropic effects cannot be entirely excluded, potentially biasing the results. Third, the analysis was conducted primarily using GWAS data from populations of European ancestry, limiting the applicability of the findings to other ethnic groups. Fourth, the assumptions underlying MR particularly that the selected instruments influence GIST risk solely through miRNA levels may not be fully testable, raising concerns about potential violations. Lastly, while the study provides evidence suggestive of causality, functional validation through experimental studies is necessary to confirm the biological mechanisms underlying these associations.

6. Conclusion

This Mendelian Randomization analysis suggests a potential causal link between microRNAs and the risk of gastrointestinal stromal tumors. By using genetic variants as instrumental variables, the study minimizes confounding and provides more reliable evidence of causality. These findings highlight the possible role of miRNAs in GIST development and their potential as biomarkers or therapeutic targets. However, limitations such as limited instrumental variables and population specificity warrant further validation. Future studies, including functional experiments and larger, diverse cohorts, are needed to confirm these associations and explore their clinical implications.

Acknowledgements: None

Funding: The study was supported by the Natural Science Foundation of Guangdong Province (Grant No. 2023A1515012548) and the Science and Technology Program of Guangzhou (Grant No. 2024A04J4802).

Availability of Data and Materials: All the data for the present article can be found on the GWAS.

Authors' Contributions: Qionglin Huang collected, analyzed, and interpreted the data, wrote the manuscript. Pengkhun Nov and Jiqiang Li designed, revised, and supervised the study. All authors had reviewed and approved the final manuscript.

Ethics Approval and Consent to Participate: Not applicable.

Patient Consent for Publication : Not applicable.

Competing Interests: The authors declare that they have no competing interests.

Reference

1. Park SH, Kim MK, Kim H, Song BJ, Chi JG. Ultrastructural studies of gastrointestinal stromal tumors. J Korean Med Sci. 2004 Apr; 19(2):234-44. doi: 10.3346/jkms.2004.19.2. 234. PMID:15082897; PMCID:PMC282 2305.
2. Niinuma T, Suzuki H, Sugai T. Molecular characterization and pathogenesis of gastrointestinal stromal tumor. Transl Gastroenterol Hepatol. 2018 Jan 9;3:2. doi: 10.21037/tgh.2018.01.02. PMID: 29441367; PMCID: PMC5803009.
3. Ghani A, Singh H, Kumar H, Vaiphei K. MicroRNA expression signature in gastrointestinal stromal tumour & their molecular & histological features. Indian J Med Res. 2024 Jul;160(1):118-127. doi: 10. 25259/ijmr_2567_22. PMID: 39382501; PMC ID: PMC11463855.
4. Kupcinskas J. Small Molecules in Rare Tumors: Emerging Role of MicroRNAs in GIST. Int J Mol Sci. 2018 Jan 30;19(2):397. doi: 10.3390/ijms19020397. PMID: 293856 88; PMCID: PMC5855619.
5. Richmond RC, Davey Smith G. Mendelian Randomization: Concepts and Scope. Cold Spring Harb Perspect Med. 2022 Jan 4;12(1): a040501. doi: 10.1101/cshperspect.a040501. PMID: 34426474; PMCID: PMC8725623.

6. Nikpay M, Beehler K, Valsesia A, Hager J, Harper ME, Dent R, McPherson R. Genome-wide identification of circulating-miRNA expression quantitative trait loci reveals the role of several miRNAs in the regulation of cardiometabolic phenotypes. Cardiovasc Res. 2019 Sep 1;115(11):1629-1645. doi: 10.1093/cvr/cvz030. PMID: 30715214.
7. Boef AG, Dekkers OM, le Cessie S. Mendelian randomization studies: a review of the approaches used and the quality of reporting. Int J Epidemiol. 2015 Apr;44(2): 496-511. doi: 10.1093/ije/dyv071. Epub 2015 May 6. PMID: 25953784.
8. Burgess S, Dudbridge F, Thompson SG. Combining information on multiple instrumental variables in Mendelian randomization: comparison of allele score and summarized data methods. Stat Med. 2016 May 20;35(11):1880-906. doi:10.1002/sim.6835. Epub 2015 Dec 13. PMID: 26661904; PMCID: PMC4832315.
9. Bowden J, Davey Smith G, Burgess S. Mendelian randomization with invalid instruments: effect estimation and bias detection through Egger regression. Int J Epidemiol. 2015 Apr;44(2):512-25. doi: 10.1093/ije/dyv080. Epub 2015 Jun 6. PMID: 26050253; PMCID: PMC4469799.
10. Hartwig FP, Davey Smith G, Bowden J. Robust inference in summary data Mendelian randomization via the zero modal pleiotropy assumption. Int J Epidemiol. 2017 Dec 1;46(6):1985-1998. doi: 10.1093/ije/dyx102. PMID: 29040600; PMCID: PMC5837715.
11. Greco M FD, Minelli C, Sheehan NA, Thompson JR. Detecting pleiotropy in Mendelian randomisation studies with summary data and a continuous outcome. Stat Med. 2015 Sep 20;34(21):2926-40. doi: 10.1002/sim.6522. Epub 2015 May 7. PMID: 25950993.
12. Burgess S, Thompson SG. Interpreting findings from Mendelian randomization using the MR-Egger method. Eur J Epidemiol. 2017 May;32(5):377-389. doi: 10.1007/s10654-017-0255-x. Epub 2017 May 19. Erratum in: Eur J Epidemiol. 2017 May;32(5):391-392. doi: 10.1007/s10654-017-0276-5. PMID: 28527048; PMCID: PMC5506233.
13. Ong JS, MacGregor S. Implementing MR-PRESSO and GCTA-GSMR for pleiotropy assessment in Mendelian randomization studies from a practitioner's perspective. Genet Epidemiol. 2019 Sep;43(6):609-616. doi: 10.1002/gepi.22207. Epub 2019 May 2. PMID: 31045282; PMCID: PMC6767464.
14. Ding F, Lai J, Gao Y, Wang G, Shang J, Zhang D, Zheng S. NEAT1/miR-23a-3p/KLF3: a novel regulatory axis in melanoma cancer progression. Cancer Cell Int. 2019 Aug 22;19:217. doi: 10.1186/s12935-019-0927-6. PMID: 31462890; PMCID: PMC6706883.
15. Zuo H, Liu S, Li X, Hou G. miR-23a-3p promotes the development of colon cancer by inhibiting the expression of NDRG4. Clin Transl Oncol. 2023 Apr;25(4):933-940. doi: 10.1007/s12094-022-02996-4. Epub 2022 Nov 14. PMID: 36374403.
16. Lu Y, Chan YT, Tan HY, Zhang C, Guo W, Xu Y, Sharma R, Chen ZS, Zheng YC, Wang N, Feng Y. Epigenetic regulation of ferroptosis via ETS1/miR-23a-3p/ACSL4 axis mediates sorafenib resistance in human hepatocellular carcinoma. J Exp Clin Cancer Res. 2022 Jan 3;41(1):3. doi: 10.1186/s13046-021-02208-x. PMID: 34980204; PMCID: PMC8722264.
17. Liu J, Fan L, Yu H, Zhang J, He Y, Feng D, Wang F, Li X, Liu Q, Li Y, Guo Z, Gao B, Wei W, Wang H, Sun G. Endoplasmic Reticulum Stress Causes Liver Cancer Cells to Release Exosomal miR-23a-3p and Up-regulate Programmed Death Ligand 1 Expression in Macrophages. Hepatology. 2019 Jul;70(1):241-258. doi: 10.1002/hep.30607. Epub 2019 Apr 25. PMID: 30854665; PMC ID: PMC6597282.
18. Peng L, Li S, Li Y, Wan M, Fang X, Zhao Y, Zuo W, Long D, Xuan Y. Regulation of BTG3 by microRNA-20b-5p in non-small cell lung cancer. Oncol Lett. 2019 Jul;18(1):137-144. doi: 10.3892/ol.2019.10333. Epub 2019 May 7. PMID: 31289482; PMCID: PMC6539950.
19. Zhang H, Zou X, Wu L, Zhang S, Wang T, Liu P, Zhu W, Zhu J. Identification of a 7-microRNA signature in plasma as promising biomarker for nasopharyngeal carcinoma detection. Cancer Med. 2020 Feb;9(3):1230-1241. doi: 10.1002/cam4.2676. Epub 2019 Dec 19. PMID: 31856390; PMCID: PMC6997065.
20. Streleckiene G, Inciuraite R, Juzenas S, Salteniene V, Steponaitiene R, Gyvyte U,

Kiudelis G, Leja M, Ruzgys P, Satkauskas S, Kupcinskiene E, Franke S, Thon C, Link A, Kupcinskas J, Skieceviciene J. miR-20b and miR-451a Are Involved in Gastric Carcinogenesis through the PI3K/AKT/mTOR Signaling Pathway: Data from Gastric Cancer Patients, Cell Lines and Ins-Gas Mouse Model. Int J Mol Sci. 2020 Jan 29;21(3):877. doi: 10.3390/ijms21030877. PMID: 32013265; PMCID: PMC7038213.

21. Qi JC, Yang Z, Zhang YP, Lu BS, Yin YW, Liu KL, Xue WY, Qu CB, Li W. miR-20b-5p, TGFBR2, and E2F1 Form a Regulatory Loop to Participate in Epithelial to Mesenchymal Transition in Prostate Cancer. Front Oncol. 2020 Jan 15;9:1535. doi: 10.3389/fonc. 20 19. 01535. PMID: 32010624; PMCID: PMC6974577.
22. Li Z, Wu L, Tan W, Zhang K, Lin Q, Zhu J, Tu C, Lv X, Jiang C. MiR-20b-5p promotes hepatocellular carcinoma cell proliferation, migration and invasion by down-regulating CPEB3. Ann Hepatol. 2021 Jul-Aug;23: 100345. doi:10.1016/j.aohep.2021.100345. Epub 2021 Mar 31. PMID: 33812045.
23. Xiang M, Yuan W, Zhang W, Huang J. Expression of miR-490-5p, miR-148a-3p and miR-608 in bladder cancer and their effects on the biological characteristics of bladder cancer cells. Oncol Lett. 2019 May;17(5):4437-4442. doi: 10.3892/ol.2019.10143. Epub 2019 Mar 12. PMID: 30988813; PMCID: PMC6447928.
24. Zhang Y, Schiff D, Park D, Abounader R. MicroRNA-608 and microRNA-34a regulate chordoma malignancy by targeting EGFR, Bcl-xL and MET. PLoS One. 2014 Mar 12;9 (3):e91546. doi: 10.1371/journal.pone.0091546. PMID:24621885; PMCID: PMC3951453.
25. Othman N, In LL, Harikrishna JA, Hasima N. Bcl-xL silencing induces alterations in hsa-miR-608 expression and subsequent cell death in A549 and SK-LU1 human lung adenocar cinoma cells. PLoS One. 2013 Dec 10;8(12):e81735. doi: 10.1371/journal.pone.0081735. PMID: 24339958; PMCID: PMC3858247.
26. Akhtar N, Makki MS, Haqqi TM. MicroRNA-602 and microRNA-608 regulate sonic hedgehog expression via target sites in the coding region in human chondrocytes. Arthritis Rheumatol. 2015 Feb;67(2):423-34. doi: 10.1002/art.38952. PMID: 25385442; PMCID: PMC4539020.
27. Gu W, Wen D, Lu H, Zhang A, Wang H, Du J, Zeng L, Jiang J. MiR-608 Exerts Anti-inflammatory Effects by Targeting ELANE in Monocytes. J Clin Immunol. 2020 Jan; 40(1):147-157. doi: 10.1007/s10875-019-00702-8. Epub 2019 Nov 20. PMID: 31749032.
28. Wang Y, Fang J, Gu F. MiR-125b-5p/TPD52 Axis Affects Proliferation, Migration and Invasion of Breast Cancer Cells. Mol Biotechnol. 2022 Sep;64(9):1003-1012. doi: 10.1007/s12033-022-00475-3. Epub 2022 Mar 23. PMID: 35320453.
29. Gołąbek K, Hudy D, Świętek A, Gaździcka J, Dąbrowska N, Miśkiewicz-Orczyk K, Zięba N, Misiołek M, Strzelczyk JK. miR-125b-5p, miR-155-3p, and miR-214-5p and Target E2F2 Gene in Oral Squamous Cell Carcinoma. Int J Mol Sci. 2023 Mar 28;24 (7):6320. doi: 10.3390/ijms24076320. PMID: 37047293; PMCID: PMC10094498.
30. Jiang M, Yang Y, Niu L, Li P, Chen Y, Liao P, Wang Y, Zheng J, Chen F, He H, Li H, Chen X. MiR-125b-5p modulates the function of regulatory T cells in tumor microenvironment by targeting TNFR2. J Immunother Cancer. 2022 Nov;10(11):e005241. doi: 10.1136/jitc-2022-005241. PMID: 36319063; PMCID: PMC9628696.
31. Wang F, Zhong S, Mao C, Jin J, Wang H. Circ_0000291 contributes to hepatocellular carcinoma tumorigenesis by binding to miR-1322 to up-regulate UBE2T. Ann Hepatol. 2022 Sep-Oct;27(5):100722. doi: 10.1016/j.aohep.2022.100722. Epub 2022 May 13. PMID: 35569812.
32. Xu C, Fan L, Lin Y, Shen W, Qi Y, Zhang Y, Chen Z, Wang L, Long Y, Hou T, Si J, Chen S. Fusobacterium nucleatum promotes colorectal cancer metastasis through miR-1322/CCL20 axis and M2 polarization. Gut Microbes. 2021 Jan-Dec;13(1):1980347. doi: 10.1080/19490976.2021.1980347. PMID: 34632963; PMCID: PMC8510564.
33. Xie T, Fu DJ, Li ZM, Lv DJ, Song XL, Yu YZ, Wang C, Li KJ, Zhai B, Wu J, Feng NH, Zhao SC. CircSMARCC1 facilitates tumor progression by disrupting the crosstalk between prostate cancer cells and tumor-associated macrophages via miR-1322/CCL20/CCR6 signaling. Mol Cancer. 2022

Sep 1;21(1):173. doi: 10.1186/s12943-022-01630-9. Erratum in: Mol Cancer. 2023 Oct 23;22(1):173. doi: 10.1186/s12943-023-01881-0. PMID: 36045408; PMCID: PMC943 4883.

34. Zhang Y, Hu SL, Hu D, Jiang JG, Cui GL, Liu XD, Wang DW. miR-1322 regulates ChREBP expression via binding a 3'-UTR variant (rs1051943). J Cell Mol Med. 2018 Nov;22 (11):5322-5332. doi: 10.1111/jcmm.13805. Epub 2018 Aug 5. PMID: 30079502; PMCID: PMC6201350.
35. Shen Y, Chen G, Gao H, Li Y, Zhuang L, Meng Z, Liu L. miR-939-5p Contributes to the Migration and Invasion of Pancreatic Cancer by Targeting ARHGAP4. Onco Targets Ther. 2020 Jan 14;13:389-399. doi: 10.2147/OTT.S227644. PMID: 32021284; PMCID: PMC6969703.
36. Nafea H, Youness RA, Abou-Aisha K, Gad MZ. LncRNA HEIH/miR-939-5p interplay modulates triple-negative breast cancer progression through NOS2-induced nitric oxide production. J Cell Physiol. 2021 Jul; 236(7):5362-5372. doi: 10.1002/jcp.30234. Epub 2020 Dec 23. PMID: 33368266.
37. Chen Y, Guo Y, Yan W. lncRNA RP5-916L7.2 correlates with advanced tumor stage, and promotes cells proliferation while inhibits cells apoptosis through targeting miR-328 and miR-939 in tongue squamous cell carcinoma. Clin Biochem. 2019 May;67:24-32. doi: 10.1016/j.clinbiochem.2019.02.013. Epub 2019 Feb 28. PMID: 30825424.
38. Zhang Y, Liu X, Li Q, Zhang Y. lncRNA LINC00460 promoted colorectal cancer cells metastasis via miR-939-5p sponging. Cancer Manag Res. 2019 Feb 22;11:1779-1789. doi: 10.2147/CMAR.S192452. PMID: 30863183; PMCID: PMC6391123.